ADA042671

TEMPERATURE, STRESS AND OPTICAL PHASE DIFFERENCE
FOR A WINDOW TRANSMITTING A CW LASER BEAM

J.L. Zar
Avco Everett Research Laboratory, Inc.
2385 Revere Beach Parkway
Everett, Massachusetts 02149

October 1976

Research Report 432

APPROVED FOR PUBLIC RELEASE;
DISTRIBUTION UNLIMITED

SECURITY CLASSIFICATION OF THIS PAGE *(When Data Entered)*

REPORT DOCUMENTATION PAGE		READ INSTRUCTIONS BEFORE COMPLETING FORM
1. REPORT NUMBER	2. GOVT ACCESSION NO.	3. RECIPIENT'S CATALOG NUMBER
4. TITLE *(and Subtitle)* Temperature, Stress and Optical Phase Difference for a Window Transmitting a CW Laser Beam		5. TYPE OF REPORT & PERIOD COVERED Research Report 432
		6. PERFORMING ORG. REPORT NUMBER
7. AUTHOR(s) J. L. Zar		8. CONTRACT OR GRANT NUMBER(s) F19628-75-C-0066
9. PERFORMING ORGANIZATION NAME AND ADDRESS Avco Everett Research Laboratory 2385 Revere Beach Parkway Everett, Massachusetts 02149		10. PROGRAM ELEMENT, PROJECT, TASK AREA & WORK UNIT NUMBERS
11. CONTROLLING OFFICE NAME AND ADDRESS Defense Advanced Research Projects Agency ARPA Order No. 2806		12. REPORT DATE October 1976
		13. NUMBER OF PAGES 21
14. MONITORING AGENCY NAME & ADDRESS*(if different from Controlling Office)* Deputy for Electronics Technology Rome Air Development Center AFSC, United States Air Force Hanscom Air Force Base, Mass. 01731		15. SECURITY CLASS. *(of this report)* Unclassified
		15a. DECLASSIFICATION/DOWNGRADING SCHEDULE

16. DISTRIBUTION STATEMENT *(of this Report)*

Approved for public release; distribution unlimited.

17. DISTRIBUTION STATEMENT *(of the abstract entered in Block 20, if different from Report)*

18. SUPPLEMENTARY NOTES

19. KEY WORDS *(Continue on reverse side if necessary and identify by block number)*

Laser window
Optical path difference
Zinc selenide

Window testing
Window distortion
Fourier Bessel transform

20. ABSTRACT *(Continue on reverse side if necessary and identify by block number)*

A crystal of CVD zinc selenide was placed in the steady 2 kW beam of a 10.6 μm laser. The beam was approximately gaussian with 1/e radius of 0.24 cm. Fifty frame per second motion pictures were taken of the time dependent optical distortion as observed with He-Ne light and a Mach-Zehnder interferometer. Thirty-one circular fringes originated in 10 seconds.

CONTINUED

DD FORM 1473 EDITION OF 1 NOV 65 IS OBSOLETE
1 JAN 73

(20)

A theoretical solution is derived for the heating rate, rate of development
of thermoelastic stress and rate of change of optical path as a function of
time, radius, and surface cooling rate. The expressions are obtained in
closed form for a gaussian laser beam and presented in non-dimensional
form. The theory is then compared with the experiment. For the first
five seconds of heating, there is good agreement. In the next four seconds,
the heating rate is higher than calculated and the discussion contains some
possible explanations.

TEMPERATURE, STRESS AND OPTICAL PHASE DIFFERENCE FOR A WINDOW TRANSMITTING A CW LASER BEAM

The transmission of a laser beam through a plane window gives rise to a change in optical path length as a result of three physical phenomena; (1) change in window thickness by heating and thermal expansion; (2) change in index of refraction as a result of heating and (3) change in both thickness and index as a result of thermoelastic stress set up by temperature gradients during the time of illumination or subsequent cooling of the window. In this paper, a solution to the optical path difference (OPD) resulting from these three mechanisms is derived in analytic form and the results applied to a window experiment where the time dependent OPD for a plane window was experimentally determined during and after illumination by a laser beam.

The problem of the time dependent heating of a laser window by an isotropic and centrally positioned laser beam has already been solved by various methods.[1, 2, 3]* In the present work the Fourier Bessel transform is used and it yields the temperature, strain, and stress distributions in closed form. The window response can thus be evaluated without the need for numerical integration methods, at least for some problems of practical importance.

A typical laser window material is isotropic with failure characteristics generally described as brittle. For an acceptable window, the absorption of laser radiation in it is sufficiently low that the transmitted beam may be approximated by an intensity distribution independent of z. The window has a radius b, a thickness, ℓ. The incident laser beam that is used is normal to the window surface and has a gaussian intensity distribution given by

$$I = P a^2 e^{-a^2 r^2}/\pi \qquad (1)$$

---

*The first two authors use finite Fourier Bessel transforms to state the problem but use numerical methods for the integrations. The third author does not employ a gaussian laser beam.

where P = laser power and a is a constant. The window has an absorption coefficient of β per cm ($\beta \ell \ll 1$) so that the heating rate in degrees per cubic cm per second is given by

$$\dot{T} = \dot{T}_o e^{-a^2 r^2} \qquad (2)$$

and

$$\dot{T}_o = \frac{\beta P a^2}{\pi \rho c} \qquad (3)$$

where ρc is the specific heat per unit volume of the laser window (assumed to be a constant). Thus far nothing has been said regarding reflections from the incident and emerging surfaces of the window. This should be considered because β is defined in terms of the intensity of radiation inside a medium. If one calculates the reduction in intensity resulting from surface reflections, and also the increase in absorption resulting from multiple internal reflections of the transmitted radiation, the two effects compensate each other.[4] One finds that the absorbed intensity $A \approx I_o \beta \ell$ independent of the reflection coefficient and the reflected intensity $R \approx 2 R_1 I_o$ independent of β (R_1 is the reflection coefficient from a single optical surface). Thus, nature has cooperated in this instance in making it unnecessary to formally include the micro details of the reflection and transmission process. All that is required in Eq. (3) is that $\beta \ell$ be small and that the two surfaces of the window be not accurately perpendicular to the wave front in order that the localized interference fringes resulting from internal reflections are spaced much closer than $1/a$ apart.

The equation leading to the temperature distribution in the window, as described, is the Fourier Heat Conduction Law.

$$\frac{\partial^2 T}{\partial r^2} + \frac{1}{r} \frac{\partial T}{\partial r} - \frac{1}{\kappa} \frac{\partial T}{\partial t} + \frac{\dot{T}}{\kappa} = 0 \qquad (4)$$

$$0 \leq r \leq b$$
$$0 \leq z \leq \ell$$

where κ is the thermal diffusivity and the last term is the heat generated per unit volume. The boundary conditions are that $\frac{\partial T}{\partial z} = 0$ at $z = 0$ and ℓ and $\frac{\partial T}{\partial r} = 0$ at $r = 0$ and b. The case where surface cooling occurs will be treated subsequently as an extension of the solution of Eq. (4).

The differential equation is solved by two calculations in which the temperature at the center is first a step function and then the solution is rewritten for a continuous central temperature. The first step makes use of the Hankel transform of order zero (also called the Fourier Bessel transform) $\overline{T}(\xi) = \int_0^\infty r\, J_0(r\xi)\, T(r, t)\, dr$.

$$\overline{T}(\xi) = A_0 \int_0^\infty r\, J_0(r\xi)\, \exp(-a^2 r^2)\, dr \tag{5}$$

where A_0 is the temperature at the center of the window, $r = 0$. The integration is given in closed form by[5]

$$\overline{T}(\xi) = (A_0/2a^2) \exp(-\xi^2/4a^2)$$

After integration, the solution is found by taking the inverse transform

$$T(r, t) = \int_0^\infty e^{-\kappa \xi^2 t}\, T(\xi)\, \xi\, J_0(\xi r)\, d\xi \tag{6}$$

$$= \left(A_0/2a^2\right) \int_0^\infty \exp\left(-\xi^2 \left[1 + 4\kappa a^2 t\right]/4a^2\right) \xi\, J_0(\xi r)\, d\xi \tag{7}$$

$$T(r, t) = \left(A_0/\left[1 + 4\kappa a^2 t\right]\right) \exp\left(-r^2 a^2/\left[1 + 4\kappa a^2 t\right]\right) \tag{8}$$

The second calculation uses the Duhamel superposition theorem[6]

$$T(r, t) = \int_0^t A_0(t)\, \frac{\partial}{\partial t}\, T(r, t - \tau)\, d\tau \tag{9}$$

and since

$$A_0(t) = \int_0^t \dot{T}_0\, d\tau = \dot{T}_0 \int d\tau = \dot{T}_0(t) .$$

$$T(r, t) = \dot{T}_0 \int_0^t \frac{\exp\left\{(-r^2 a^2/\left[1 + 4\kappa a^2 (t - \tau)\right]\right\}}{1 + 4\kappa a^2 (t - \tau)}\, d\tau \tag{10}$$

This integrates to[7]

$$T(r, t) = \left(\dot{T}_0/4\kappa a^2\right)\left[\mathrm{Ei}\left(-r^2 a^2\right) - \mathrm{Ei}\left(-\frac{r^2 a^2}{1 + 4\kappa a^2 t}\right)\right] \tag{11}$$

Here Ei(x) is the exponential integral of negative arguments, tabulated in Jahnke and Emde[8] as the function $Ei(x) = -\int_x^\infty t^{-1} \exp(-t)\,dt$. (Abramowitz[5] calls this function $-E_1(x)$).

Equation (11) gives in closed form, the time and radial dependence of the heating of a window by a laser beam of gaussian intensity profile when the window is larger than the laser beam, there is negligible heat loss from surfaces and edges and there is negligible reduction in laser intensity as a result of internal absorption. Figure 1 is a plot of the non-dimensional temperature rise $T/\dot{T}_o\, t$ against the non-dimensional window radius ra, as given in Eq. (11).

Window Stress and Strain

The stress and strain in a window transmitting a laser beam of gaussian intensity can also be stated in closed form. The basic equations are those for solid cylinders.[9] If the window is thicker than the laser beam mean radius, one should use the long cylinder expressions (plane strain) rather than the thin plate formulae (plane stress) because the latter theory ignores axial stress. Since failure of brittle materials occurs where the shear is a maximum, the thin plate theory leads to the conclusion that windows are stronger than they, in fact, are because the axial stress terms are the largest of the principle stresses. The equations for plane strain are:

$$(1-\nu)\,\sigma_r/aE = (1/b^2)\int_o^b T r\,dr - (1/r^2)\int_o^r T r\,dr \tag{12}$$

$$(1-\nu)\,\sigma_\theta/aE = (1/b^2)\int_o^b T r\,dr + (1/r^2)\int_o^r T r\,dr - T \tag{13}$$

$$(1-\nu)\,\sigma_z/aE = (2\nu/b^2)\int_o^b T r\,dr - T \tag{14}$$

In the above, a is the linear coefficient of expansion, E is the elastic modulus, ν is Poisson's ratio; σ is strain and 2b is the diameter of the window. These expressions contain $\int_o^r T r\,dr$ which fortunately is integrable from Eq. (11).

-4-

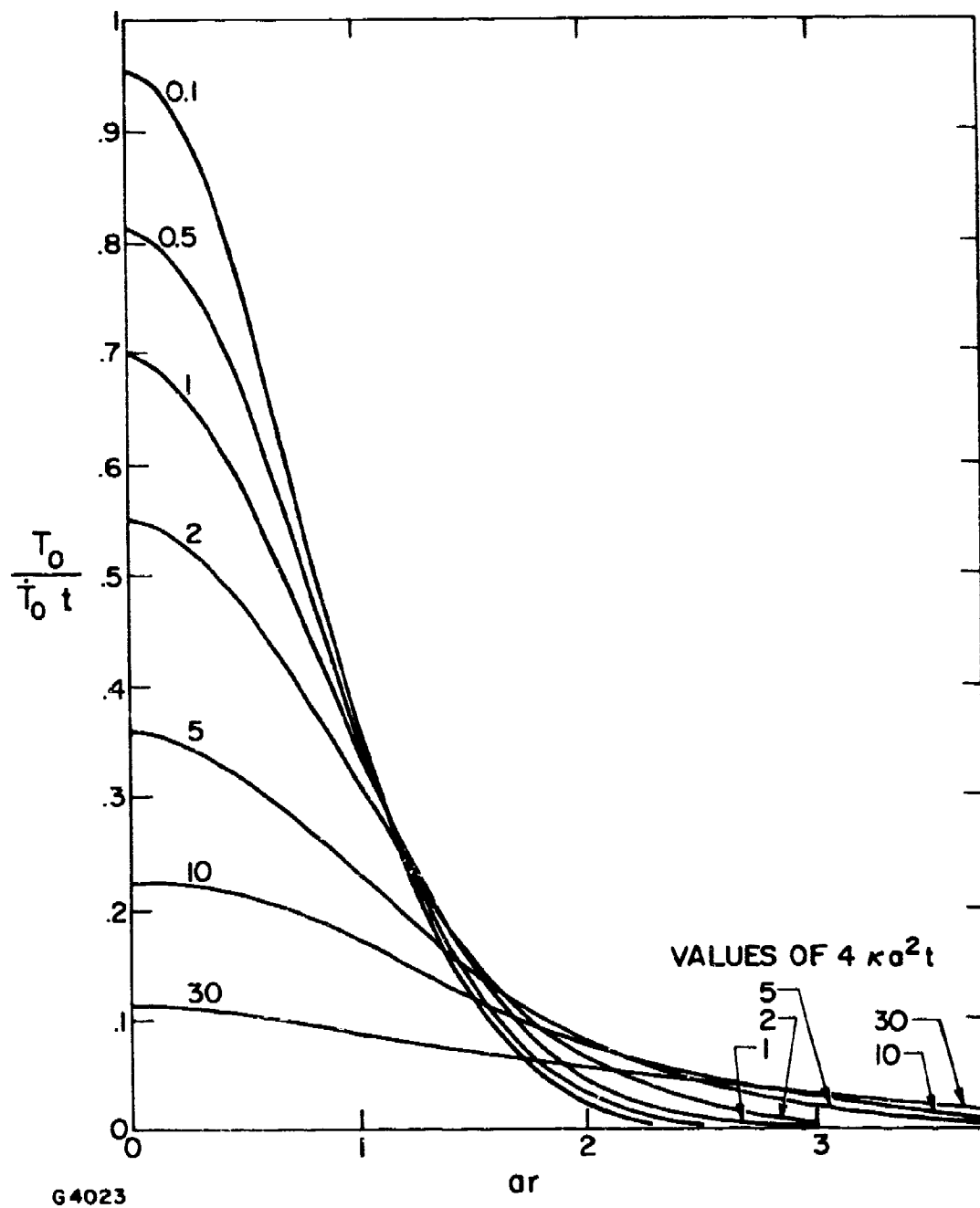Figure 1   Temperature Profiles

G4023

$$\int_o^r \text{Trdr} = \frac{\dot{T}_o}{2a^2 t} - \frac{\dot{T}_o}{8\kappa a^4} \left[(1 + 4\kappa a^2 t)\, e^{-\frac{r^2 a^2}{1+4\kappa a^2 t}} - e^{-r^2 a^2} \right]$$

$$+ \frac{\dot{T}_o}{8\kappa a^4} \left[\text{Ei}(-r^2 a^2) - \text{Ei}\left(\frac{-r^2 a^2}{1+4\kappa a^2 t}\right) \right] \tag{15}$$

The $\int_o^b \text{Trdr}$ has a much simpler physical significance. It is proportional to the total energy absorbed in the window and therefore can be related to the incident laser power.

$$\int_o^b \text{Trdr} = \frac{\beta Pt}{2\pi\rho c} = (b^2/2)\, T_1 \tag{16}$$

where T_1 is the temperature rise for infinitely high window conductivity and is a constant for a particular experiment.

Upon substituting the expressions (15) and (16) into the stress Eqs. (12) to (14) it follows that

$$\frac{2(1-\nu)\sigma_r}{\alpha ET} = \frac{\dot{T}_o t}{T}\left(\frac{1}{a^2 b^2} - \frac{B}{a^2 r^2}\right) - 1 \tag{17}$$

$$\frac{2(1-\nu)\sigma_\theta}{\alpha ET} = \frac{\dot{T}_o t}{T}\left(\frac{1}{a^2 b^2} + \frac{B}{a^2 r^2}\right) - 1 \tag{18}$$

$$\frac{2(1-\nu)\sigma_z}{\alpha ET} = 2\frac{\dot{T}_o t}{T}\frac{\nu}{a^2 b^2} - 2 \tag{19}$$

where

$$B = 1 + \frac{\exp(-r^2 a^2) - (1+4\kappa a^2 t)\exp\left(-\frac{r^2 a^2}{1+4\kappa a^2 t}\right)}{4\kappa a^2 t}$$

Figures 2, 3 and 4 are plots of the non-dimensional radial, tangential and axial stresses respectively

$$S_{r,\theta,z} = \left(\frac{T}{\dot{T}_o t}\right)\left(4\kappa a^2 t\right)\left(\frac{2[1-\nu]\sigma_{r,\theta,z}}{\alpha ET}\right) \tag{20}$$
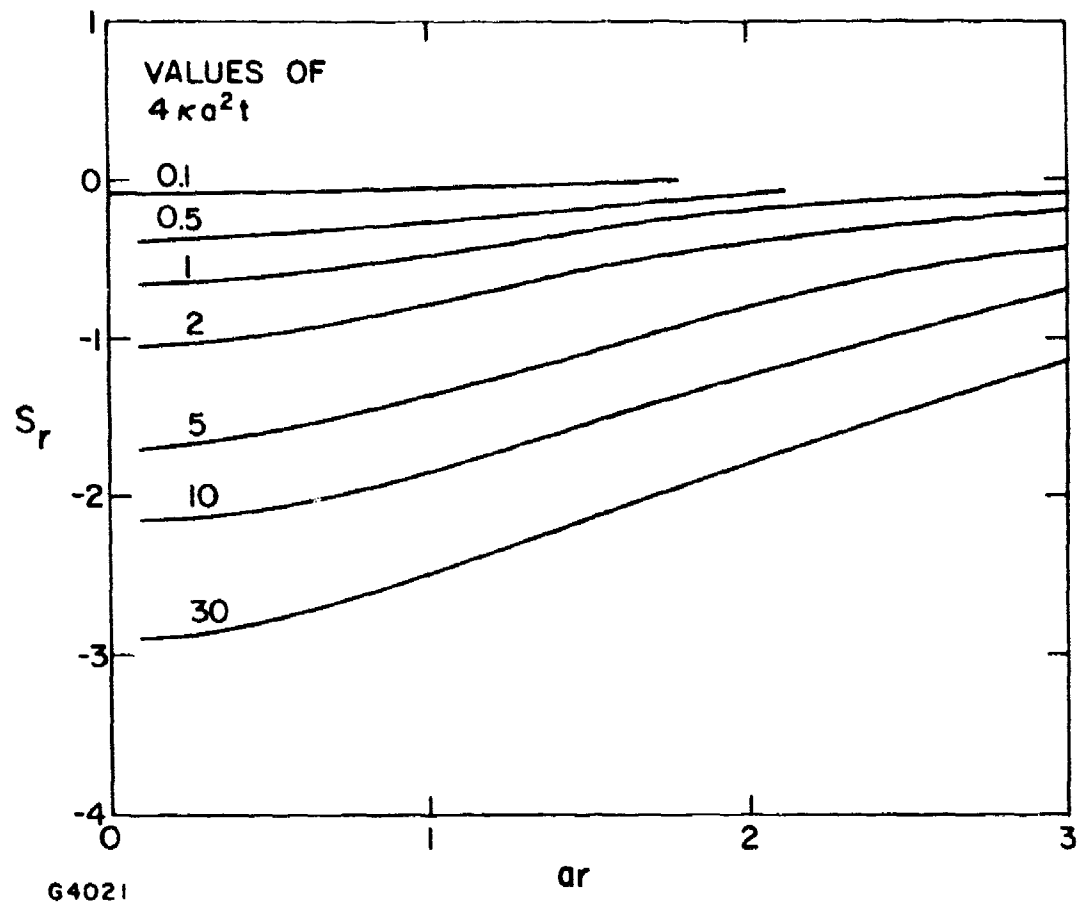
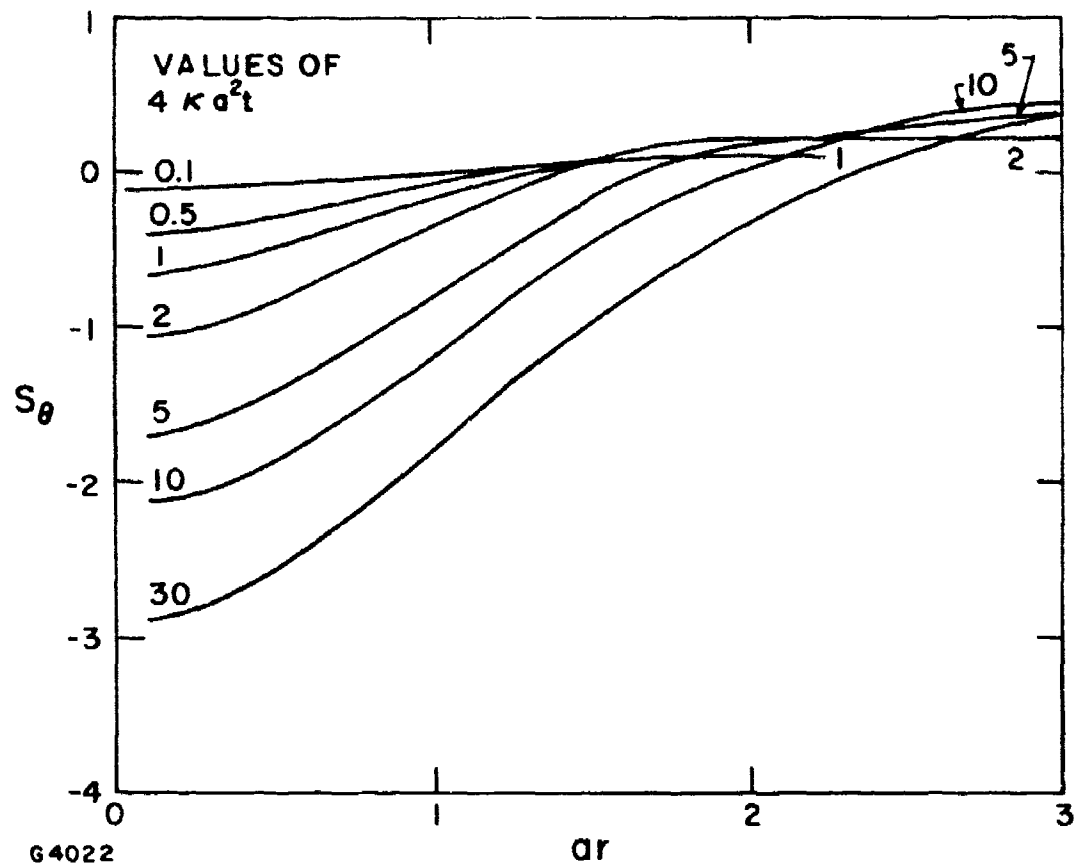Figure 2   Non-Dimensional Radial Stress

G4021
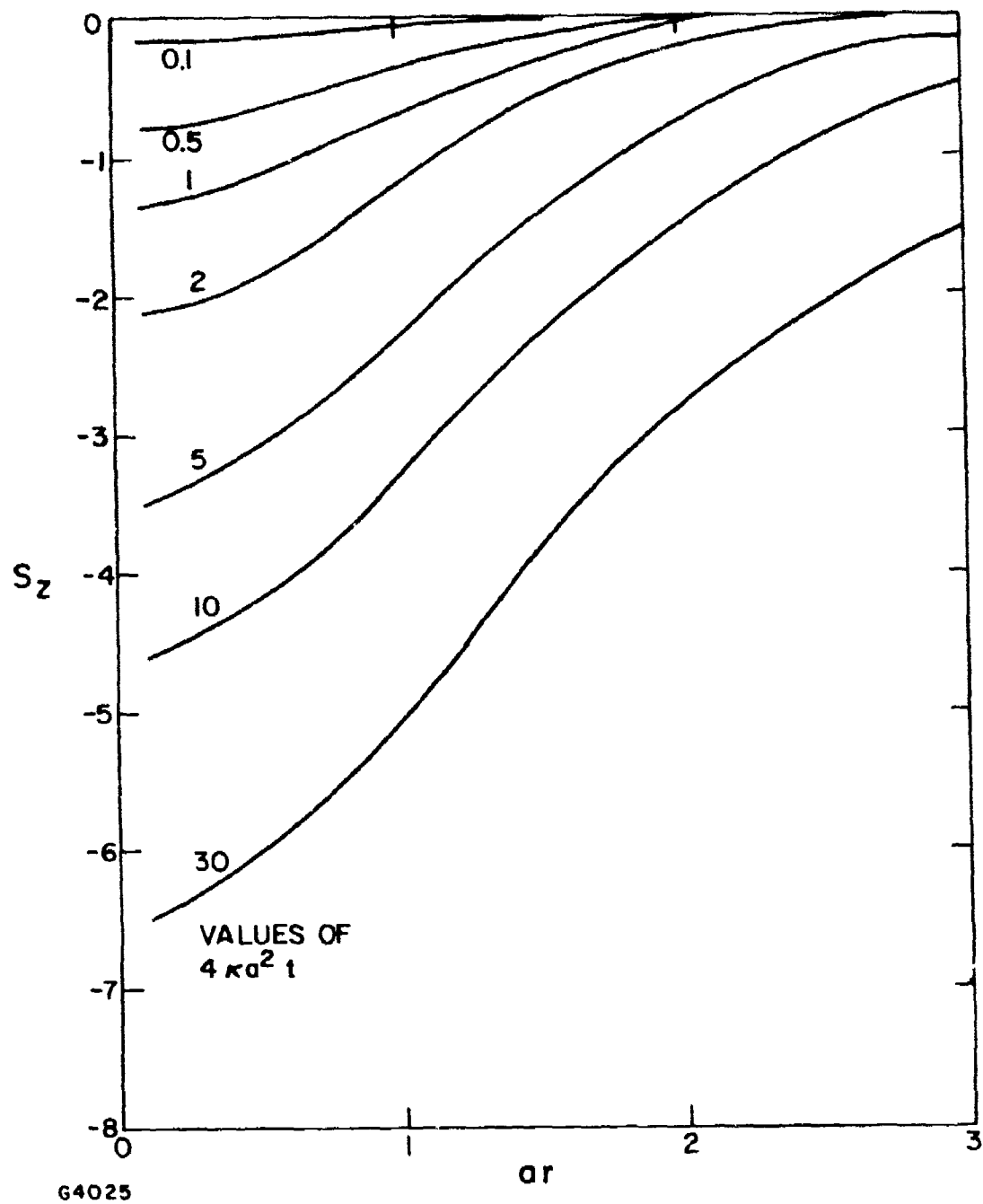
Figure 3   Non-Dimensional Tangential Stress

Figure 4   Non-Dimensional Axial Stress

G4025

From which the individual stress values may be obtained for an experiment by

$$\sigma_{r,\,\theta,\,z} = \frac{S_{r,\,\theta,\,z}\,\beta P\alpha E}{8\pi\kappa\rho c\,(1-\nu)} \tag{21}$$

It can be seen from these curves that the axial stress is about twice as large as the others.

The axial strain for a thin cylinder (plane stress) is given by

$$\epsilon_z = \alpha T + \sigma_z/E - \nu\,(\sigma_r + \sigma_\theta)/E \tag{22}$$

The plane stress equations are

$$\sigma_r = \alpha E\left[T_1/2 - (1/r^2)\int_0^r Trdr\right]$$

$$\sigma_\theta = \alpha E\left[T_1/2 + \left(1/r^2\right)\int_0^r Trdr - T\right]$$

$$\sigma_z = 0. \tag{23}$$

These lead to the expression for axial strain when the laser beam nearly completely fills the window

$$\epsilon_z = \alpha T + \nu\alpha\,(T - T_1)$$

For cylinders that are thicker than the laser beam radius one uses the stress Eqs. (12) to (14) but in addition, one should rewrite Eq. (22) by replacing E by $E/(1-\nu^2)$; ν by $\nu/(1-\nu)$ and α by $\alpha(1+\nu)$.[9] This leads to the thick window expression for axial strain.

$$\epsilon_z = \alpha\,\frac{1+\nu}{1-\nu}\left[T + \nu\,(T - T_1)\right] \tag{24}$$

In terms of non-dimensional quantities, one has the non-dimensional axial strain

$$E_z = \frac{4\pi(1-\nu)}{(1+\nu)^2}\,\frac{\rho c\kappa}{\beta P\alpha}\,\epsilon_z = \left[1 - \frac{\dot{T}_o t}{T}\,\frac{\nu}{\nu+1}\,\frac{1}{a^2 b^2}\right]\frac{T}{\dot{T}_o t}\,(4\kappa a^2 t) \tag{25}$$

In early stages of window heating, the second term in the bracket may be neglected compared to 1 so that

$$E_z \approx \frac{T}{\dot{T}_o t} \ (4\kappa a^2 t) \tag{26}$$

This is plotted in Figure 5 for various values of the non-dimensional radius and transmission time.

Failure

In triaxial loading of brittle materials, failure occurs when the maximum shear stress equals half the yield stress, σ_y, as determined in a uniaxial test. [10]

There are three maxima of shear which occur at 45 degrees to the principle stress directions. We expect failure when

$$\tau = \pm \frac{1}{2} \text{Max} (\sigma_1 - \sigma_2) = \frac{1}{2} \sigma_y$$

where σ_1 and σ_2 are any of the three principle stresses taken in whatever order gives the largest τ. Since the axial stress is approximately twice the other stresses, failure is predicted when $\sigma_z \approx 2\sigma_y$ and this first occurs on the central axis of the laser beam. The max shear stress is plotted in Figure 6.

Optical path changes in a plane window that is heated by a laser beam was observed by including the window in one leg of a Mach Zehnder interferometer. [4] The dependence of the OPD on the temperature is found by evaluating the individual contributions of several phenomena.

$$\text{OPD} = \Delta n \ell = \int_o^T n_s \frac{d\ell}{dT} \ dT + \int_o^T \ell_s \frac{dn}{dT} \ dT \tag{27}$$

where n_s is the index of refraction as customarily measured at zero stress, ℓ is the window thickness and ℓ_s is the thickness measured at zero stress. Through the use of Eq. (24),

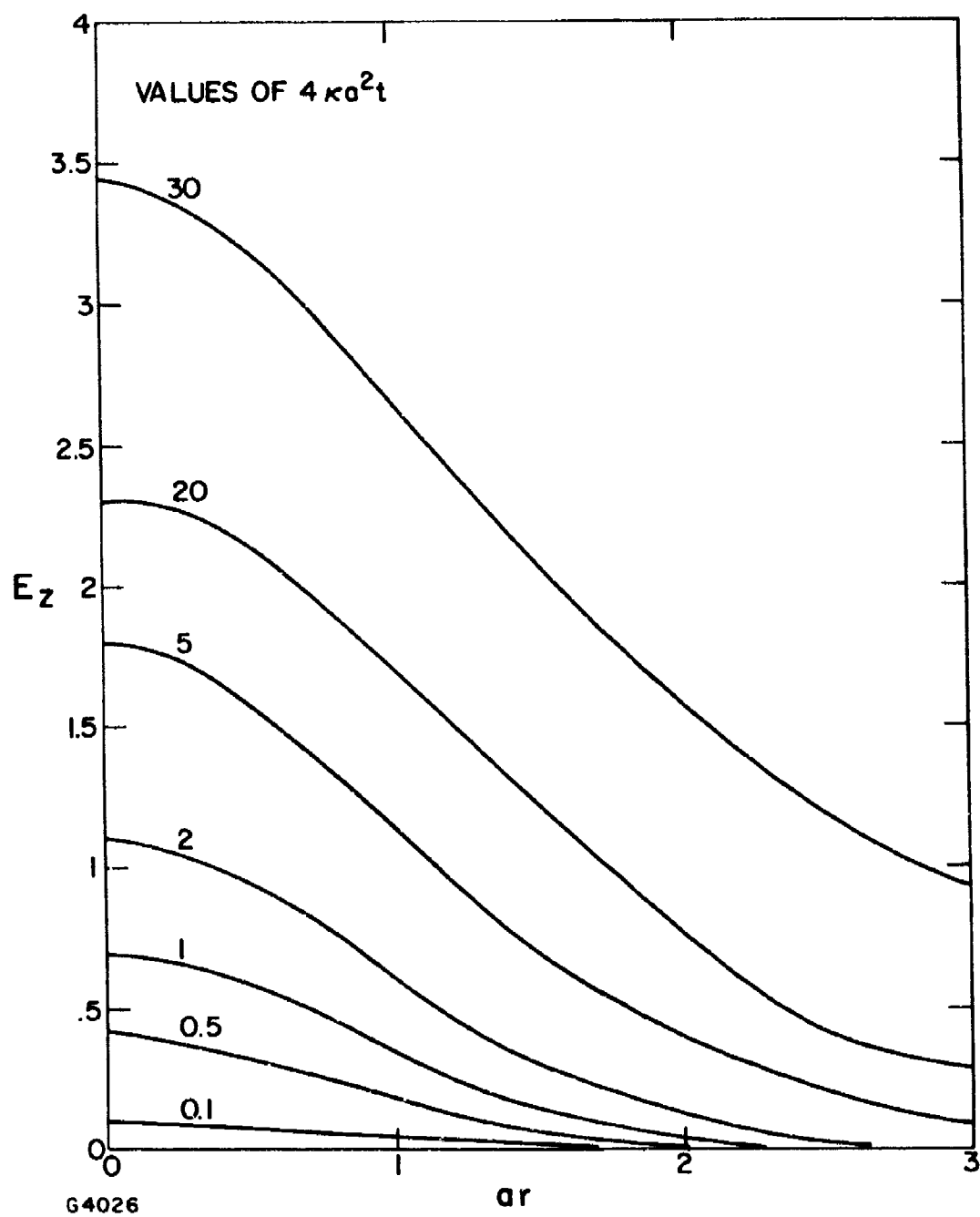$$\frac{d\ell}{dT} = \ell \ \frac{d\epsilon_z}{dT} = \ell \ \frac{(1+\nu)^2}{1-\nu} \ \alpha_s \tag{28}$$
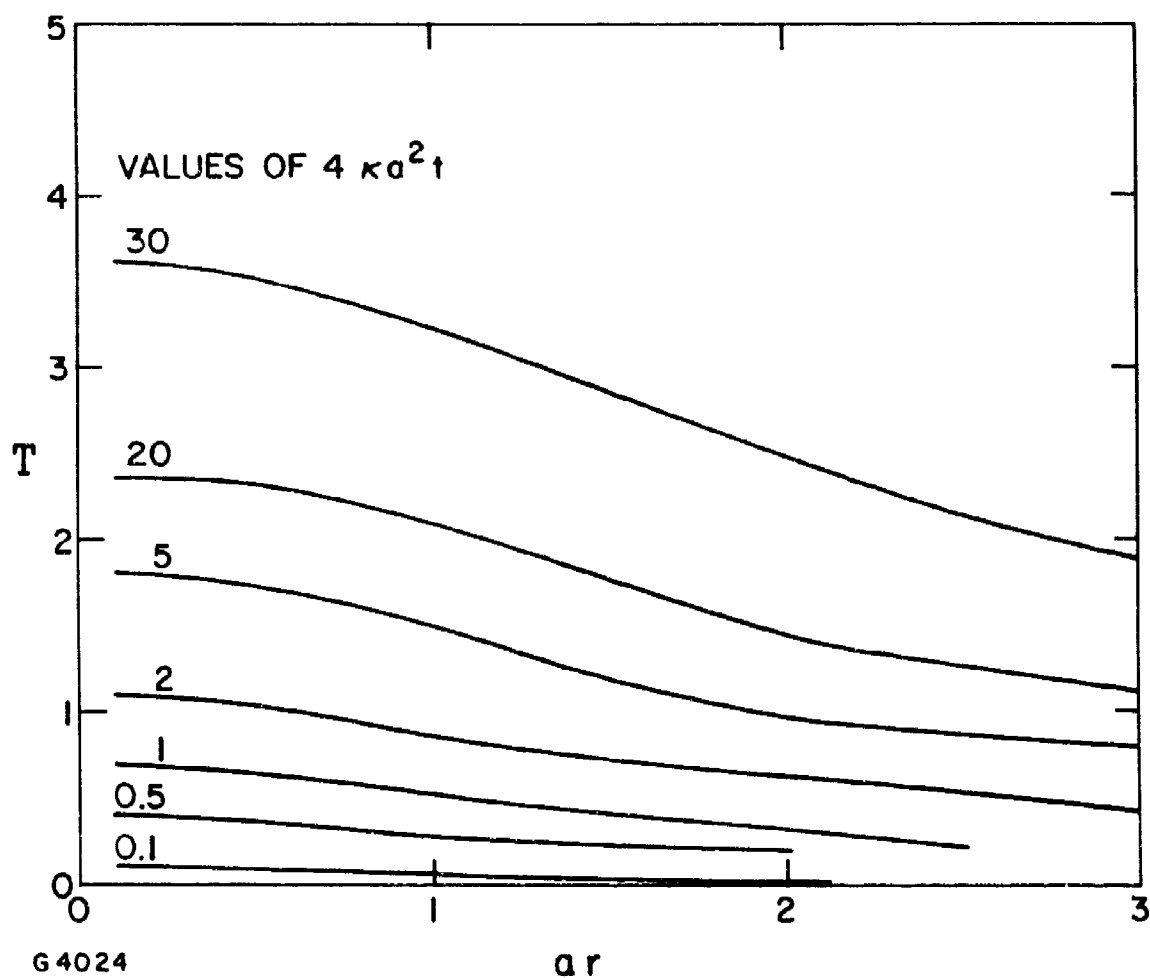
Figure 5   Non-Dimensional Strain

G4026

Figure 6   Non-Dimensional Maximum Shear Stress

G 4024

Here, α_s is the coefficient of expansion as measured at zero stress. It is to be noted that Eq. (28) already includes the thermal expansion term even in the absence of temperature induced strains. Also,

$$\frac{dn}{dT} = \frac{\partial n}{\partial \sigma} \frac{d\sigma_r}{dT} + \frac{dn}{\partial \sigma_\theta} \frac{d\sigma_\theta}{dT} + \frac{\partial n}{\partial \sigma_z} \frac{d\sigma_z}{dT} + \frac{dn_s}{dT} \tag{29}$$

The last term in Eq. (29) is required because there is a change in index of refraction with temperature even when the temperature is uniform and there is zero thermoelastic stress. Following the usual classical derivation of stress birefringence, one has for cubic crystals[11] transmitting a plane wave in the z direction,

$$\frac{1}{n_s^2} - \frac{1}{n^2} = q_{11} \sigma_z + q_{12} (\sigma_r + \sigma_\theta) \approx \frac{2}{n_s^2} \frac{\partial n}{\partial \sigma} d\sigma \tag{30}$$

Here q_{11} and q_{12} are the stress optic coefficients. $q_{11} = \frac{\partial n}{\partial \sigma_z}$ and $q_{12} = \frac{\partial n}{\partial \sigma_r} = \frac{\partial n}{\partial \sigma_\theta}$.

$$\frac{dn}{dT} = \frac{2}{n^2} \left[q_{11} \frac{d\sigma_z}{dT} + q_{12} \frac{d}{dT} (\sigma_r + \sigma_\theta) \right] + \frac{dn_s}{dT} \tag{31}$$

The derivatives of the stresses are obtained from Eqs. (17) to (19). The evaluation of these stress-optic terms is very simple for cubic crystals because the B term is not present in either σ_z or in the sum $(\sigma_r + \sigma_\theta)$.

$$\frac{d\sigma_z}{dT} = \frac{d(\sigma_r + \sigma_\theta)}{dT} = -\frac{\alpha E}{1-\nu}$$

$$\text{OPD} = \frac{T\ell}{1-\nu} \left[(1 + \nu)^2 \alpha_s - \frac{2\alpha_s E}{n_s^2} (q_{11} + q_{12}) + (1 - \nu) \frac{dn_s}{dT} \right] \tag{32}$$

Note that the last term in the bracket of Eq. (32) is often the dominant term.

Surface cooling of windows through the use of a flushing gas stream
is an effective method of removing laser beam generated heat. This is
particularly useful for windows with antireflection coatings because a large
part of the window heating may originate in the surface and it is efficient
to remove it at the source.

Equation (4) is now expanded to include a term for removal of heat
from two surfaces with a surface heat transfer coefficient, h W/cm^2 deg.

$$\frac{\partial^2 T}{\partial r^2} + \frac{1}{r}\frac{\partial T}{\partial r} - \frac{1}{\kappa}\frac{\partial T}{\partial t} + \frac{\dot{T}}{\kappa} - \frac{2hT}{k\ell} = 0 \tag{33}$$

The solution to this equation proceeds in a similar way to that for Eq. (4);
that is, by first finding a solution for a steady step addition of heat by a
gaussian source, ($\dot{T}/\kappa = 0$ in Eq. (33)) and then applying the Duhamel
superposition integral to calculate the result for a time dependent, con-
tinuous heat source.[8] Equation (33) becomes

$$\frac{\partial^2 T}{\partial r^2} + \frac{1}{r}\frac{\partial T}{\partial r} - \frac{1}{\kappa}\frac{\partial T}{\partial t} = h' T \tag{34}$$

where $h' = 2h/k\ell$. The solution for the step heat addition, corresponding
to Eq. (8) is

$$T_o(r, t) = \left[\dot{T}^*/(1 + 4\kappa a^2 t)\right] \exp\left[-\kappa h' t\right] \exp\left[-r^2 a^2/(1 + 4\kappa a^2 t)\right] \tag{35}$$

In the above $\dot{T}^*$ is a temperature change at $r = 0$ which will be evaluated
shortly. This equation is now inserted in Eq. (9)

$$T(r, t) = \dot{T}^* \int_o^t \frac{\exp\left[-\kappa h'(t-\tau)\right] \exp\left[-r^2 a^2/\left[1+\kappa a^2 (t-\tau)\right]\right]}{1 + 4\kappa a^2 (t-\tau)} d\tau \tag{36}$$

The integration is performed by expanding the first exponential in a power
series $\exp\left[-\kappa h' (t-\tau)\right] \approx 1 - \kappa h' (t-\tau) + \ldots$. For the experiment that we
will try to explain, the $\kappa h' t \ll 1$ for $t \ll 100$ sec and therefore only the first
two terms of the expansion are sufficient at early times. This gives two
terms to the integral of Eq. (36) $T(r, t) = T_1 + T_2$. T_1 is identical to
Eq. (10) for which the solution is stated in Eq. (11). This also permits
identification of $\dot{T}^*$ as identical to $\dot{T}_o$.

T_2 can be found in closed form by integration by parts.

$$T_2(r, t) = \dot{T}_o \frac{\kappa h'}{(4\kappa a^2)^2} \left\{ \exp\left[-r^2 a^2\right] - (1 + 4\kappa a^2 t) \exp\left[-r^2 a^2/(1 + 4\kappa a^2 t)\right] \right.$$

$$\left. + (1 + r^2 a^2)\left[Ei\left[-r^2 a^2\right] - Ei\left[-r^2 a^2/(1 + 4\kappa a^2 t)\right]\right] \right\}$$

The complete solution of Eq. (36) is thus obtained by adding Eq. (11)

$$T(r, t) = \frac{\dot{T}_o}{4\kappa a^2} \left\{ \left[1 + \frac{h'(1 + r^2 a^2)}{4a^2}\right]\left[Ei(-r^2 a^2) - Ei\left(\frac{-r^2 a^2}{1 + 4\kappa a^2 t}\right)\right] \right.$$

$$\left. + \frac{h'}{4a^2}\left[\exp(-r^2 a^2) - (1 + 4\kappa a^2 t)\exp\left(-\frac{r^2 a^2}{1 + 4\kappa a^2 t}\right)\right] \right\} \qquad (37)$$

where $\kappa h' t \ll 1$. On the axis, $(r = 0)$ this equation must be restated to remove the indeterminate form.

$$\lim_{r=0} T(r, t) = \frac{\dot{T}_o}{4\kappa a^2}\left[\ln(1 + 4\kappa a^2 t)\left(1 + \frac{h'}{4a^2}\right) - 4\kappa a^2 t \frac{h'}{4a^2}\right] \qquad (38)$$

Comparison with an experiment. In an experiment, using a CW laser beam at the Laser Window Test Facility[4] a window of uncoated CVD zinc selenide was exposed for 10 seconds to a 2 kW laser beam with an approximate gaussian intensity distribution. A detailed description of the experimental procedure is being published elsewhere.[14] In brief, the distortion of the window produced by heating was observed by taking 50 frame per second motion pictures of Mach-Zehnder interference fringes during and after exposure to the laser beam using a helium neon laser source to illuminate the interferometer. During and subsequent to the exposure, the two faces of the window were surface cooled by flat jets of nitrogen gas with an estimated surface heat transfer coefficient of 0.0124 W/cm^2 deg C. Other pertinent data pertaining to this experiment are given in Table I.

By analysis of the motion pictures, a curve of fringe count versus exposure time was obtained for the OPD on the center line of the laser

TABLE I

EXPERIMENTAL DATA FOR THE CVD Zinc Se TEST

Window diameter	$2b$	$= 3.6$ cm
Window thickness	ℓ	$= .82$ cm
Laser beam power	P	$= 2$ kW
Beam mean diameter	$1/a$	$= .24$ cm
Surface heat transfer coefficient	h	$= .0124$ W/cm^2 deg
He-neon laser wavelength	λ	$= 6.33 \times 10^{-5}$ cm
Nominal absorption coefficient	β	$= .005$ cm^{-1}
Poisson's ratio[12]	ν	$= .28$
Elastic modulus[12]	E	$= 6.9 \times 10^{11}$ d/cm^2
Index of refraction[12]	n_s	$= 2.403$
Temp. coef. of n[12]	dn_s/dT	$= 7.9 \times 10^{-5}$ deg^{-1}
Stress birefringence[12]	q_{11}	$= -1.39 \times 10^{-13}$ cm^2/dyne
	q_{12}	$= 0.58 \times 10^{-13}$ cm^2/dyne
Volumetric specific heat[13]	ρc	$= 2.65$ J/cm^3 deg
Thermal diffusivity[13]	κ	$= .0491$ cm^2/sec
Thermal expansion coef.[13]	α	$= 7.2 \times 10^{-6}$ deg^{-1}
Yield stress[13]	σ_y	$= 5.6 \times 10^8$ dyne/cm^2

beam. This is plotted in Figure 7. Superimposed on this curve is a plot of the theoretical Eq. (32) evaluated by use of the data in Table I. The window was supplied to us by AFCRL and it was stated that the previous measured value of β was $0.005/cm^{-1}$.

The correction term to the laser power, for surface cooling, according to Eq. (38) is evaluated first. After 9 seconds, it is 0.985 and at shorter times it is even closer to 1.0. Therefore, it is considered to be negligible.

The OPD is found from Eq. (32). The first term in the bracket (thermal expansion) is 1.18×10^{-5} deg^{-1}. The second term (stress optic effect) is 13.9×10^{-7} deg^{-1}. The third term (change in index) is 5.69×10^{-5} deg^{-1} and is the dominant one.

Discussion. Comparison of the calculated and experimentally measured curves of Figure 7 shows that the theory accurately predicts the OPD up to the first 5 seconds of heating. After 10 seconds the theoretical curve is about 15% below the observed curve and has a smaller slope. There are three possible explanations for this discrepancy. The central portion of the window has been heated about 25 degrees in 10 seconds. It is possible that some of the properties of CVD zinc selenide, besides n_s, have a temperature dependence which is not accounted for in the calculations. The most likely property to have a temperature dependence is β, which in the present theory is assumed to be constant. Skolnik, et al., calculated the temperature dependence of β on the assumption that it is due to multiphonon absorption[15] and stated that there could be a 33% increase in β over a 25 degree temperature change. However the authors measurements of β for the samples which they possessed was independent of temperature over the range from 300 to 500 $^{\circ}$C. Therefore, it is not likely that a β dependence on T is the correct explanation.

Another possible cause of the discrepancy at long heating times is that the present theory assumes an infinitely large window with a centrally heated region. In actuality, the laser beam center was about 0.7 cm from the edge of the window. The heated zone would have diffused to the edge in 5 seconds after which time the window temperature would rise faster in this experiment than for a much larger window. The extent of
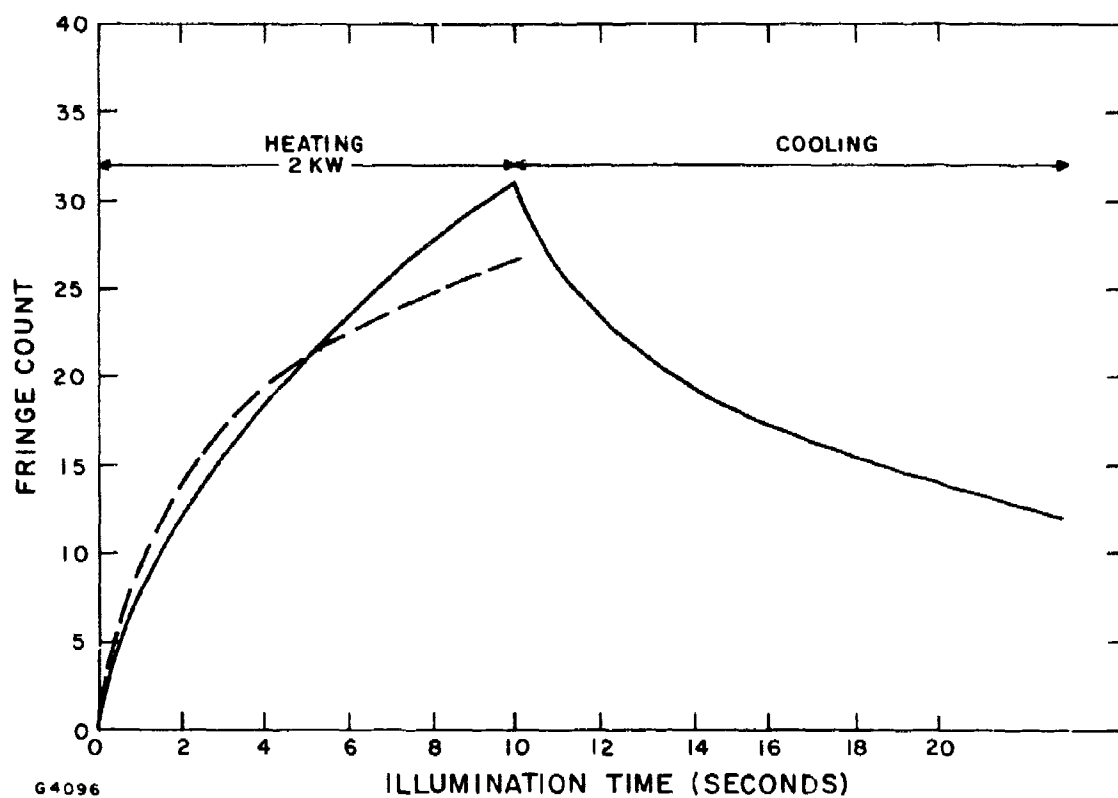
Figure 7   Comparison of Experimental and Calculated Optical
Path Difference

the extra heating may be estimated by interpolation of Figure 1 at $ra = 0$ and $4\kappa a^2 t = 22$ and 44 corresponding to 5 and 10 seconds of heating. The temperature of a large window should have risen by 50% for a 100% increase in the time. For a smaller window, with a smaller diffusion area, after 5 seconds there would be a smaller increase in temperature. This is qualitatively sufficient to explain the difference between the observed and theoretical heating curves at long heating times. The third explanation is that the value of α may not have been accurately measured. We have calculated that for the conditions of the experiment, $dT/T = -3.24\, d\alpha/\alpha$. Thus a 15% error in T could be accounted for by a 5% error in the knowledge of α. We believe that a portion of the discrepancy at long heating times may be ascribed to this cause also.

REFERENCES

1. Glickler, S. L., Thermal Stress Analysis of Windows and Mirrors Due to Axisymmetric Laser Heating, Avco Research Report 410, August 1975.

2. Bernal, G. E., Heat Flow Analysis of Laser Absorption Calorimetry, Applied Optics 14, 314 (1975).

3. Carslaw, H. S. and Jaeger, J. C., Conduction of Heat in Solids, Oxford University Press (1959) especially Section 17.2.

4. Zar, J. L., Semiannual Technical Report No. 2, Investigations into the Feasibility of High Power Laser Window Materials, AFCRL-TR-75-0605, Oct. 1975.

5. Abramowitz, M. and Stegun, I. A., Handbook of Mathematical Functions, Bureau of Standards, Applied Mathematics Series 55 (1964) Chapter 11.

6. Arpaci, V. S., Conduction Heat Transfer, Addison Wesley (1966).

7. Sutton, G. W., Private Communication.

8. Jahnke, E. and Emde, F., Tables of Functions, Dover Publications (1965).

9. Timoshenko, S. and Goodier, J. N., Theory of Elasticity, McGraw-Hill (1951), especially Chapter 14.

10. Roark, R. J., Formulas for Stress and Strain, McGraw-Hill Book Co. (1965).

11. Born, M. and Wolf, E., Principles of Optics (Pergamon).

12. Feldman, A., Malitson, I. H. and Horowitz, D., Optical Properties of Polycrystaline Zinc Selenide. Proceedings 4th Annual Laser Window Damage Conference - 1974, p. 117.

13. Dickinson, S. K., Infrared Laser Window Materials Property Data AFCRL-TR-75-0318 (1975).

14. Zar, J. L., Investigations into the Feasibility of High Power Laser Window Materials, Semiannual Technical Report No. 3, April 1976. To be published.

15. Skolnik, L. N., Lipson, H. G., Bendow, B. and Schott, J. T., Appl. Phys. Lett. 8, 442, (1974).